DEUTSCHES ELEKTRONEN-SYNCHROTRON DESY

DESY 86-055
June 1986

ELECTROWEAK BOSON SELF-COUPLINGS AND THE SCALE OF COMPOSITENESS

by

J.A. Grifols, S. Peris

Dept. de Física Teórica, Univ. Autônoma de Barcelona, Bellaterra

J. Solà

Deutsches Elektronen-Synchrotron DESY, Hamburg

ISSN 0418-9833

NOTKESTRASSE 85 · 2 HAMBURG 52

To be sure that your preprints are promptly included in the HIGH ENERGY PHYSICS INDEX , send them to the following address (if possible by air mail) :

DESY
Bibliothek
Notkestrasse 85
2 Hamburg 52
Germany

DESY 86-055
June 1986

ISSN 0418-9833

ELECTROWEAK BOSON SELF-COUPLINGS AND THE SCALE OF COMPOSITENESS*

J.A. Grifols and S. Peris

Departament de Física Teórica
Universitat Autónoma de Barcelona
BELLATERRA, Barcelona (Spain)

J. Solà

Deutsches Elektronen-Synchrotron
DESY, Hamburg

ABSTRACT: The experimental constraint on $\delta\rho=\frac{\delta M_W^2}{M_W^2}-\frac{\delta M_Z^2}{M_Z^2}$ and the experimental rate of the process $K_L\to\mu\mu$ are used to bound hypothetical non-standard self interactions of the electroweak bosons. In particular, we give bounds on anomalous magnetic dipole and electric quadrupole moments of the charged weak boson.

*.- Work partially supported by reasearch project CAICYT.

1.- INTRODUCTION

The direct experimental check of the nonabelian gauge nature of the vector boson couplings of electroweak theory is still lacking. LEP II will have direct access to the ZWW and γWW vertices but until then probably no direct experimental handle on this important issue will be available. Meanwhile, only indirect probes of these couplings are possible. In fact, already existing, low energy experiments allow to put constraints on the actual structure of those vertices. Specifically, the muon anomaly has been used to limit the magnetic dipole moment and electric quadrupole moment of the charged weak boson $W^{\pm}$ [1]. Also, low energy $\nu e\to\nu e$ and $\bar{\nu}e\to\bar{\nu}e$ scattering data supply interesting information on those quantities [2]. The resulting bounds are, given the precision of present data, not very restrictive. But an improved experiment as the newly proposed BNL (g-2) experiment should result in an order of magnitude improvement of those bounds. Interestingly enough another source of information on gauge boson self-couplings are the mass shifts to weak boson masses (relative to the radiative corrected standard model values) or, equivalently, the deviations from unity of the ρ-parameter. In this latter instance, however, the conclusions that can be drawn from the existing literature are inconsistent. On the one hand, some authors [3-4] find constraints to the parameters in the boson vertices which are comparable to the ones found otherwise (e.g. $(g-2)_\mu$) . But, Suzuki, using the same input data obtains extremely stringent bounds on the anomalous magnetic dipole moment of the charged weak boson [5]. Indeed, this author finds: $\Delta\chi<7\times10^{-3}\,|1/\Lambda^4(\mathrm{TeV})|$. Whereas in refs.(3-4) one finds a quadratic dependence in the compositeness scale and $\Delta\chi<O(.1\text{-}1)$ for Λ=1 TeV.

The purpose of the present paper is to analyse those questions more thoroughly. In section 2 we present the framework and discuss the strategy. Section 3 is devoted to numerical results on the γWW and ZWW parameters as derived from the experimental limits on the ρ-parameter . In the next two sections we expand further on the analysis of the ZWW coupling. Indeed, in section 4 we confront a very general phenomenological ZWW vertex

with the experimental data on the parameter ρ. Data on $K_L \to \mu\mu$ provides further insight on the ZWW vertex. This is dealt with in sect. 5. Unfortunately, the bounds derived from $K_L \to \mu\mu$ are very poor. Finally, section 6 contains a brief summary of results.

2.- FRAMEWORK

If the W and Z bosons are composite this fact will obviously reflect itself in radiative effects that depart from the standard higher order corrections. In particular, the masses of the weak bosons and their relative magnitude should show sensible deviations from what one expects in the standard model. These deviations, however, are constrained by experiment . Therefore, one can hopefully obtain useful information on substructure by demanding that such effects do not exceed the experimentally allowed values.

The amplitudes that lead to corrections of the masses of the weak bosons (which involve 3 and 4 boson self-coupling vertices) are shown in fig. 1. They contribute to the vacuum polarization functions of the gauge bosons. Even if the couplings in fig. 1 were standard $SU(2)\times U(1)$ couplings, the amplitudes as they stand are ill-defined. In fact, these self-energy diagrams are UV-divergent. Now, it is important for our purposes to perfectly separate what would be genuine effects of substructure -i.e. divergent behaviour which is cut-off by a momentum Λ linked to new structure and which has a true physical content- from the UV behaviour which is conveniently removed by renormalization of a few free parameters in the theory. Electroweak theory contains three basic parameters which are to be fixed by experiment. They might be the Fermi constant G_F , the fine-structure constant α, and Weinberg's angle $s^2 \equiv \sin^2\theta_W$ (any other choice would do). The experimental extraction of these parameters can be carried out with the help of three low energy processes such as 1) muon decay, 2) Coulomb scattering, and 3) neutral scattering involving neutrinos. This is the approach which we shall follow here in order to insure consistent results when we go to the standard model limit.[6] Once we guarantee finite results for the mass shifts δM_W^2 and δM_Z^2 in the standard model we can try to estimate how much do possible deviations from gauge structure of the boson self-couplings contribute to those shifts. When we perform the loop integrals, involving couplings which are only pointlike when probed over distances large on the scale of Λ^{-1}, we shall allow only for momenta up to the cut-off Λ (the hypothesized new scale of compositeness). Higher momenta will be damped by form factors linked to the new level of compositeness. Although this procedure has a clear physical justification, it obviously will break gauge invariance in the symmetric limit and therefore render nonsensical results when one goes to the standard model limit. For this reason, our strategy will be to split our vertex functions into a standard plus a non-standard piece and do the calculations (cut-off-integrals) only with the second piece. By calculating only deviations from the standard results we automatically ensure a smooth transition to the standard model results for the radiative shifts to M_W^2 and M_Z^2.

Let us now briefly sketch the renormalization process that we mentioned before[6].

To lowest order we have,

$$\frac{G_F}{\sqrt{2}} = \frac{g^{(0)2}}{8M_W^{(0)2}} \tag{1}$$

$$\alpha = \frac{g^{(0)2}s^{(0)2}}{4\pi} \tag{2}$$

and

$$\frac{1}{4}(1+\xi) = s^{(0)2} \tag{3}$$

where $\xi = -a^{(0)}/b^{(0)}$ with a and b beeing the neutral current coupling strengths in the neutral current lagrangian

$$\mathcal{L}_Z = \frac{g}{4c}\,\bar{l}\gamma^\mu(a-b\gamma_5)lZ_\mu \ , \quad l=e,\mu,\ldots, \ c\equiv\cos\theta_W \tag{4a}$$

To lowest order,

$$a^{(0)} = -1+4s^{(0)2} \tag{4b}$$

$$b^{(0)} = -1 \tag{4c}$$

To one loop, we have the corrected version of eqs. (1), (2) and

(3):

$$\frac{G_F}{\sqrt{2}} = \frac{g^{(1)^2}}{8M_W^2}(1+\delta_1) \tag{5}$$

$$\alpha = \frac{g^{(1)^2}s^{(1)^2}}{4\pi}(1+\delta_2) \tag{6}$$

$$\frac{1}{4}(1+\xi) = s^{(1)^2}(1-\delta_3) \ . \tag{7}$$

The different δ_i are the shifts induced by the one-loop radiative corrections to the amplitudes for the three low energy processes 1), 2) and 3) mentioned before.

As already stated, these corrections are plagued with infinities which, in the standard model limit can be renormalized away. We choose to subtract the infinities "on mass shell", i.e. the weak boson propagators are bound to have a pole at the physical mass. It is easy to check, using the above eqs. and the "on mass shell" substraction condition, that[6],

$$\delta M_W^2 = M_W^{(0)^2}(\delta_1-\delta_2-\delta_3)\Big|_{q^2=0} + \Pi_W(q^2=M_W^2) \tag{8}$$

and

$$\delta M_Z^2 = M_Z^{(0)^2}\left(\delta_1-\delta_2+\frac{s^2-c^2}{c^2}\,\delta_3\right)_{q^2=0} + \pi_Z(q^2=M_Z^2) \tag{9}$$

We shall use these formulae to compute the contribution to the mass shifts induced by non-standard weak boson couplings. In this way we ensure the correct standard model limit. Furthermore, when computing the different terms that go into eqs. (8) and (9) we shall separate them, as explained before, into two components. One component is an exclusively standard model contribution . The other extra component measures the deviations from elementarity of the intermediate gauge bosons. This latter piece is what we are really interested in, and the one which we shall explicitly work out and confront with experiment. Having stated precisely the procedure let us turn to the actual calculations.

The electromagnetic interactions for a spin 1 charged particle were systematically studied by Aronson in ref. (7). We

generalize his results to include the interactions of the Z° boson with the charged weak bosons. This is really necessary to ensure the standard model limit. Following Aronson we define a lagrangian density that allows for arbitrary anomalous magnetic moment and electric quadrupole moment,

$$\mathcal{L} = \mathcal{L}_1 + \mathcal{L}_2 + \mathcal{L}_3 \tag{10}$$

where

$$\mathcal{L}_1 = -\frac{1}{2}\hat{G}^\dagger_{\mu\nu}\hat{G}^{\mu\nu} - M_W^2 W^\dagger_\mu W^\mu - \frac{1}{2}M_Z^2 Z_\mu Z^\mu \tag{11a}$$

$$\mathcal{L}_2 = -\frac{1}{4}\sum_{i=\gamma,Z}\hat{F}_{\mu\nu_i}\hat{F}_i^{\mu\nu} \tag{11b}$$

and

$$\mathcal{L}_3 = \sum_{i=\gamma,Z}\frac{ig_i\lambda_i}{M_W^2}\hat{F}_{\mu\nu}{}^i\hat{G}^{\dagger\mu\rho}\hat{G}^\nu_\rho \tag{11c}$$

with

$$\hat{G}_{\mu\nu} \equiv (\partial_\mu - ig_\gamma A_\mu - ig_Z Z_\mu)W_\nu - (\partial_\nu - ig_\gamma A_\nu - ig_Z Z_\nu)W_\mu \tag{12}$$

and

$$\hat{F}^i_{\mu\nu} \equiv F^i_{\mu\nu} + ig_i\chi_i(W^\dagger_\mu W_\nu - W^\dagger_\nu W_\mu) \tag{13}$$

In eq. (12) and (13), the $F_{\mu\nu}$ and g_i are given by,

$$F^\gamma_{\mu\nu} = \partial_\mu A_\nu - \partial_\nu A_\mu$$

$$F^Z_{\mu\nu} = \partial_\mu Z_\nu - \partial_\nu Z_\mu$$

$$g_\gamma \equiv gs = e$$

$$g_Z \equiv gc$$

The magnetic and electric quadrupole moments are

$$\mu_i = (1+\chi_i-\lambda_i)g_i/2M_W \tag{14}$$

$$Q_i = -(\lambda_i+\chi_i)g_i/M_W^2 \tag{15}$$

The derivation of the Feynman rules for the 3 and 4 point interactions is straightforward. In table 1 we supply the relevant 3 and 4 vertices which we are going to use in our calculations. As shown, we have split each vertex into a standard piece plus an extra anomalous piece.

Now that the basic artillery is ready we shall use it.

3.- LIMITS ON THE PARAMETERS $\chi_{\gamma,Z}$ AND $\lambda_{\gamma,Z}$

Our task will be to evaluate the non-standard contributions to δ_1, δ_2, δ_3 and $\Pi_{W,Z}(q^2=M^2_{W,Z})$ entering formulas (8) and (9) exactly as prescribed in the previous section. Two types of diagrams contribute to δ_i as exemplified in fig. 2: vacuum polarization diagrams and vertex correction diagrams. Since $\delta\rho = (\delta M_W^2/M_W^2)-(\delta M_Z^2/M_Z^2)$, δ_1 and δ_2 do not contribute to this quantity.

Our results depend on four parameters, i.e. χ_γ, χ_Z, λ_γ and λ_Z. In order not to confuse matters unnecessarily, and given that the magnetic and electric quadrupole moments are a priori uncorrelated, we shall independently saturate the experimental errors on ρ with $\delta\rho$ calculated first with $\chi_{\gamma,Z}\neq 1$ and $\lambda_{\gamma,Z}=0$ and later on with $\chi_{\gamma,Z}=1$ and $\lambda_{\gamma,Z}\neq 0$. This should provide reasonably safe bounds -barring fortuitous cancellations- to both anomalous magnetic dipole and electric quadrupole moments.

Case a

We start this analysis by making $\lambda_\gamma=\lambda_Z=0$ and allow for $\chi_{\gamma,Z}\neq 1$. We have checked by explicit calculations that the vacuum polarization functions produce the main contributions to $\frac{\delta M_W^2}{M_W^2} - \frac{\delta M^2 Z}{M^2 Z}$. Consequently, we shall report only on those contributions. In this approximation -neglecting all but vacuum polarization effects- $\delta\rho$ reads,

$$\delta\rho = \frac{\Delta\pi_W(M_W^2)}{M_W^2} - \frac{\Delta\pi_Z(M_Z^2)}{M_Z^2} - \left\{\frac{s}{c}\,\frac{\Delta\pi_{Z\gamma}(q^2)}{q^2}\right\}_{q^2=0} \qquad (16)$$

Here, $\Delta\pi$ are meant to be the departures from the corresponding standard model functions. The diagrams that contribute to $\Delta\pi_W$, $\Delta\pi_Z$ and $\Delta\pi_{Z\gamma}$ are of the kind displayed on fig. 1. An explicit calculation using the Feynman rules of table 1 renders

$$\Delta\pi_W(q^2=M_W^2) = \frac{3g^2}{32\pi^2}\left[s^2\Delta\chi_\gamma+(1+c^2)\Delta\chi_Z\right]\Lambda^2+O(\log\Lambda) \qquad (17)$$

$$\Delta\pi_Z(q^2=M_Z^2) = 0+O\left[(\Delta\chi)^2\Lambda^2\right]+O(\log\Lambda) \qquad (18)$$

$$\Delta\pi_{Z\gamma}(q^2=0) = 0+O\left[(\Delta\chi)^2\Lambda^2\right]+O(\log\Lambda) \qquad (19)$$

where we kept only the terms linear in $\Delta\chi_{\gamma,Z}$.

We note in passing, that a Λ^4 dependence which is present in the individual diagrams, cancels exactly when summing the amplitudes containing the 3-vertices and the ones containing the 4-vertices.

The current experimental limit on $\delta\rho$ is $|\delta\rho|<3\%$. We shall allow for eq. (16) supplemented with eqs. (17-19) to saturate this experimental bound (the standard radiative corrections lie well below the present precision and we neglect them). Thus, combining these various pieces of information we finally get,

$$\left|s^2\Delta\chi_\gamma+(1+c^2)\Delta\chi_Z\right|<5\times10^{-2}\left(\frac{1\,\text{TeV}}{\Lambda(\text{TeV})}\right)^2 \qquad (20)$$

The numerical results obtained are given in fig. 3. The allowed region in parameter space $(\Delta\chi_\gamma,\Delta\chi_Z)$ is shown for a compositeness energy scale Λ=1 TeV. It is clear from eq. (20) and from fig. 3 that the bounds obtained are more than one order of magnitude worse than those advocated by Suzuki [1] and they are quadratic in the cutoff instead of quartic.

Case b

Consider now the case $\Delta\chi_{\gamma,Z}=0$ and $\lambda_{\gamma,Z}\neq 0$. Going through the same steps as before but using the Feynman rules in table 1 with $\Delta\chi_{\gamma,Z}=0$ and $\lambda_{\gamma,Z}\neq 0$, one obtains for the relevant vacuum polarization functions,

$$\Delta\pi_W(q^2)=\frac{q^2}{8\pi^2}\left\{\frac{\Lambda^4}{4}\left[e^2\frac{\lambda_\gamma^2}{M_W^4}+g_Z^2\frac{\lambda_Z^2}{M_W^4}\right]+3\Lambda^2\left[e^2\frac{\lambda_\gamma}{M_W^2}+g_Z^2\frac{\lambda_Z}{M_W^2}\right]\right\} + O(\log\Lambda) \qquad (21)$$

$$\Delta\pi_Z(q^2) = \frac{q^2}{8\pi^2}\,g_Z^2\left[\frac{\lambda_Z^2\Lambda^4}{4M_W^4}+3\Lambda^2\frac{\lambda_\gamma}{M_W^2}\right] + O(\log\Lambda) \qquad (22)$$

and

$$\Delta\pi_{Z\gamma}(q^2) = \frac{q^2}{16\pi^2}\,eg_Z\left[\frac{\lambda_\gamma\lambda_Z}{2M_W^4}\Lambda^4+3\left\{\frac{\lambda_\gamma}{M_W^2}+\frac{\lambda_Z}{M_W^2}\right\}\Lambda^2\right]+O(\log\Lambda) \qquad (23)$$

These eqs. are to be fed into eq. (16) to give $\delta\rho$. The resulting relation is,

$$\delta\rho = \frac{e^2}{32\pi^2}\left(\frac{\lambda_\gamma}{M_W^2}-\frac{\lambda_Z}{M_W^2}\right)\left[\Lambda^4\frac{\lambda_\gamma}{M_W^2}+6\Lambda^2\right] \qquad (24)$$

Again, we can use the 3% experimental bound on $|\delta\rho|$ to obtain limits on the parameters λ_γ and λ_Z. The permitted area in the $(\lambda_\gamma,\lambda_Z)$-plane is shown in fig. 4 for Λ=1 TeV. Actually, this figure is the combined result of using the constraint on $|\delta\rho|$ as given above and the constraint on the mass shifts $\frac{\delta M^2_{W,Z}}{M^2_{W,Z}}$ themselves (using collider data for the mass values). Of course, to do that, it was necessary to estimate also,the δ_1 and δ_2 pieces contributed by the corrections to muon decay and Coulomb scattering. In particular, the photon polarization function $\Delta\pi_\gamma(q^2)$ was needed. Its explicit form is given by the following formula,

$$\Delta\pi_\gamma(q^2) = \frac{q^2e^2}{8\pi^2}\left[\frac{\lambda_\gamma^2}{4M_W^4}\Lambda^4 + 3\frac{\lambda_\gamma}{M_W^2}\Lambda^2\right] + O(\log\Lambda) \qquad (25)$$

4.- MORE ON THE ZWW COUPLING

In the preceding sections we have treated the photon and the Z°-boson on equal footing. However, since in the present work we entertain the possibility that the intermediate weak bosons $W^\pm$ and Z° are composite objects, this might not be the most conveninet thing to do. Indeed, while the photon should still be considered a gauge particle , in our philosophy this is no longer true for the Z° boson. Let us, therefore, consider a situation where we further relax the constraints on the triple boson vertex ZWW.

We recall that in the standard model the ZWW vertex reads,

$$iV_{\alpha\beta\mu}=ig_Z\{g_{\alpha\beta}(p+p')_\mu+g_{\alpha\mu}(q-p)_\beta-g_{\beta\mu}(q+p')_\alpha\} \qquad (26)$$

This vertex contains a part which is generated by applying the minimal coupling prescription

$$\partial_\mu \to \partial_\mu - ig_Z Z_\mu \qquad (27)$$

in the kinetic term,

$$-\frac{1}{2}(\partial_\mu W_\nu-\partial_\nu W_\mu)^\dagger(\partial^\mu W^\nu-\partial^\nu W^\mu) \qquad (28)$$

and a piece which arises from a term in the lagrangian which is

$$ig_Z\chi_Z W^\dagger_\mu W_\nu(\partial^\mu Z^\nu-\partial^\nu Z^\mu) \qquad (29)$$

with χ_Z=1.

Consequently, apart from allowing for a coeficient $\chi\neq1$ in eq. (29) (this intyoduced the deviations $\Delta\chi_Z$ discussed in case a of section 3) one may envisage also a case when even the minimal substitution rule is violated. The vertex is the written as,

$$iV_{\alpha\beta\mu}=ig_Z\{g_{\alpha\beta}f_1(p+p')_\mu-f_2(g_{\alpha\mu}p_\beta+g_{\beta\mu}p'_\alpha)\} \qquad (30)$$

Eq. (30) is derived from the lagrangian density

$$\mathcal{L}_{ZWW}=ig_Z\{f_1[W^\dagger_\nu\partial^\mu W^\nu-\partial^\mu W^{\dagger\nu}W_\nu]Z_\mu-f_2[W^\dagger_\mu\partial^\mu W^\nu-\partial^\mu W^{\dagger\nu}W_\mu]Z_\nu\} \qquad (31)$$

Minimal coupling, as prescribed by eqs. (27) and (28), is achieved for $f_1=f_2=1$.

If we add to $\mathcal{L}_{ZWW}$ (eq. (31)) the term given by eq. (29) we get

$$iV_{\alpha\beta\mu}=ig_Z\{g_{\alpha\beta}(p+p')_\mu+g_{\alpha\mu}(q-p)_\alpha-g_{\beta\mu}(q+p')_\alpha+\Delta f_1 g_{\alpha\beta}(p+p')_\mu-$$

$$-\Delta f_2(g_{\alpha\mu}p_\beta+g_{\beta\mu}p'_\alpha)+\Delta\chi_Z(g_{\alpha\mu}q_\beta-g_{\beta\mu}q_\alpha)\} \qquad (32)$$

where $\Delta f_i=f_i-1$.

We have conveniently split, as usual, eq. (32) into the standard model vertex (eq. (26)) and an extra anomalous term which quantifies the departures from the SU(2)×U(1) model.

Notice at this point that eq. (31) is exactly the ZWW lagrangian used by Suzuki in ref. (1). Yet, this is not the most general C, P, T conserving interaction. To this interaction one may still add arbitrary quadrupole terms parametrized by dimensional constants λ/M^2 as in $\mathcal{L}_3$ in eq. (10). We will turn to this point later. For the moment, let us bound the new parameters Δf_1 and Δf_2.

Using vertex (32) (with $\Delta\chi_Z=0$) we evaluate the vacuum polarization function $\Delta\pi_W$, $\Delta\pi_Z$ and $\Delta\pi_{Z\gamma}$. The explicit results are, keeping only terms proportional to $\Delta f_i\Lambda^4$ and $(\Delta f_i)^2\Lambda^6$,

$$\frac{\Delta\pi_W(M_W^2)}{M_W^2} = \frac{g_Z^2c^2}{64\pi^2}\left\{\frac{1}{2}(\Delta f_2-4\Delta f_1)\frac{\Lambda^4}{M_W^4} - \frac{1}{3}\,\Delta f_{12}\frac{\Lambda^6}{M_W^6}\right\} \tag{33a}$$

where

$$\Delta f_{12} \equiv \Delta f_1-\Delta f_2 = f_1-f_2 \ . \tag{33b}$$

$$\frac{\Delta\pi_Z(M_Z^2)}{M_Z^2} = \frac{g_Z^2}{16\pi^2}\left\{\left[\Delta f_1-(1+3c^2)\Delta f_2\right]\frac{\Lambda^4}{2M_W^4} - \frac{c^2}{3}\,\Delta f_{12}^2\frac{\Lambda^6}{M_W^6}\right\} \tag{34}$$

and

$$\frac{\Delta\pi_{Z\gamma}(q_Z^2)}{q^2} = \frac{eg_Z}{64\pi^2}\,\Delta f_{12}\frac{\Lambda^4}{M_W^4} \tag{35}$$

Two brief comments on eq. (35) are necessary. First, the mixed vacuum polarization function $\pi_{\gamma Z}(q^2)$ involves, of course, the γWW coupling. We used the standard model vertex. Second, in order to maintain the transversality of the vacuum polarization tensor $\pi^{\mu\nu}{}_{\gamma Z}$ it has been necessary to add, when computing $\Delta\pi_{\gamma Z}(q^2)$ a seagull diagram, involving a 4-point vertex (see fig. 1b). Otherwise, eq. (35) would exhibit an extra spurious term proportional to q^{-2}. This term would make formula (16) infinite.

Eq. (16), when feeded with the previous results, leads to the inequality

$$\left|(1+c^2+4c^4)\Delta f_1-(1+c^2+7c^4)\Delta f_2-c^4\Delta f_{12}^2\frac{\Lambda^2}{M_W^2}\right| < 1.8\times10^{-3}\left(\frac{1\text{TeV}}{\Lambda\,(\text{TeV})}\right)^4 \tag{36}$$

once the experimental bound on $\delta\rho$ is used.

The numerical analysis of this relation is given in fig. (5). The plot shows the allowed area (shaded area) in the Δf_1, Δf_2 plane for Λ=1TeV.

Finally, for the sake of completeness, let us consider the purely phenomenological ZWW-vertex with arbitrary quadrupole and dipole terms added,

$$\begin{aligned} iV_{\alpha\beta\mu}(p,p',q) = ig_Z\{&g_{\alpha\beta}(p'+p-\theta_a p'qp+\theta_a pqp')_\mu-\theta_b p'_\mu q_\alpha p_\beta+\\ &+\theta_b p_\mu p'_\alpha q_\beta-g_{\alpha\mu}(p-\chi q-\theta_c p'qp+\theta_d p'pq)_\beta-\\ &-g_{\beta\mu}(p'+\chi q+\theta_c pqp'-\theta_d p'pq)_\alpha\} \end{aligned} \tag{37}$$

where

$$\theta_{a,b,c,d} \equiv \frac{\lambda_{a,b,c,d}}{M_W^2} \ .$$

Note that in eq. (37) we respect minimal coupling, admit anomalous magnetic dipole moment χ and, as advertised, allow for the $\frac{\lambda}{M_W^2}$ terms which we neglected before. This vertex is C, P and T conserving. One recovers the Aronson vertex (see table 1) when all λ_i are equal. Recall that in this case we found that both the $\Delta\chi_Z$ and λ_Z terms contributed to $\delta\rho$ quadratically in Λ (see eqs. (20) and (24)). In the present case, however, we shall find Λ^6 and Λ^4 terms. In fact, assuming χ=1 for simplicity, one finds after tedious but straightforward calculation involving the various vacuum polarization functions (cf. eq. (16)),

$$\delta\rho = \frac{g_Z^2}{\pi^2M_W^2}\left\{\frac{\Lambda^6\Delta\theta_Z}{192}\left(-\frac{1}{3}-\frac{c^2}{6}+\frac{4}{c^2}\right)-\Lambda^4\Delta\theta_Z\left(\frac{7}{96}+\frac{c^2}{192}+\frac{1}{24}\,\frac{s^2}{c^2}\right)\right\} \tag{38}$$

where $\Delta\theta_Z$ stands for $\theta_b-\theta_a$, $\theta_c-\theta_b$, $\theta_c-\theta_d$ which we take to be equal (again for simplicity; the exact formulas do not provide more insight and are considerably more cumbersome). This will suffice for our purposes. Notice that $\delta\rho$ is proportional to the differences $\Delta\theta_i$. This means that when all θ_i are equal the contribution from those quadrupole terms only enters at the Λ^2 order as we stressed before.

Just to have a feeling for the bounds that one gets from the experimental requirement $\delta\rho<3\%$ on the quantity $\Delta\lambda_Z=M_W^2\Delta\theta_Z$ we give a few numbers,

$-4.5\times10^{-4}<\Delta\lambda_Z<4.7\times10^{-4}$ for Λ = 1 TeV

$-7\times10^{-7}<\Delta\lambda_Z<7\times10^{-7}$ for Λ = 5 TeV

and

$-4.6\times10^{-8}<\Delta\lambda_Z<4.6\times10^{-8}$ for Λ = 10 TeV

5.- $K_L \to \mu\mu$ AND THE ZWW COUPLING

To complete the study on the ZWW coupling let us investigate a further instance where one could probe this vertex.

We propose to study the process $K_L \to \mu\mu$. Mainly for two reasons. In the first place, this is a rare process. Rare processes have led in the past to stringent constraints on model building. Moreover, since this process proceeds through virtual loops, one is able to probe the shortest distances even though the actual process is a low energy reaction.

The amplitude that describes the decay is shown in fig. 6. It involves the mechanism $K_L \to \gamma\gamma \to \mu\mu$. Yet, there are other potential amplitudes contributing. One of them contains the ZWW vertex. As shown in fig. 7 the s and d quarks in the K_L state make a 1-loop transition into the Z° boson which then decays into a $\mu\mu$ pair. This amplitude, however, is suppressed by the GIM mechanism and, furthermore, by a partial cancellation that occurs between this amplitude and the box amplitude involving virtual W^+W^- exchange [8]. Thus, the contributions from weak boson exchanges are numerically small in the standard model. Therefore, the process $K_L \to \mu\mu$ goes mainly via the $\gamma\gamma$ intermediate state and one understands (in the standard model) the smallness of its width relative to $K_L \to \gamma\gamma$. But there is no reason a priori, if substructure emerges at some energy scale, for the ZWW interaction to be exactly as prescribed by the SU(2)×U(1) theory. To the extent that large momenta contribute to the loop in fig. 7, $K_L \to \mu\mu$ might well feel the effects of compositeness. Here, we would like to infer just from the experimental rates on $K_L \to \mu\mu$ how much is the ZWW coupling allowed to depart from its standard model form.

In calculating the amplitude shown in fig. 7 we assume that the charged weak currents are conventional standard model fermion currents. Only the ZWW coupling is assumed to be anomalous. This implies that the GIM mechanism is operative here. Therefore, the bounds derived will be very conservative. As to the ZWW vertex, we shall allow for $\chi_Z \neq 1$, for $\lambda_Z \neq 0$ (and even for various λ_i as before) and for $f_1 \neq f_2$ (violation of minimal coupling). Let us consider those contributions in turn.

The amplitude associated to the $\Delta\chi_Z$ term in the ZWW vertex turns out to be proportional to

$$\varepsilon = \frac{(m_c^2 - m_u^2)\,\Delta\chi_Z}{M_W^2 \tan^2\theta_W} \frac{m_K^2}{M_W^2} \log \frac{\Lambda^2}{M_W^2} \tag{39}$$

this is extremely small and consequently gives no useful limit on the parameter $\Delta\chi_Z$.

Consider now the effect on the $s\bar{d} \to \mu\mu$ amplitude of the λ_i terms in ZWW (cf. eq. (37)). It is easy to realize that the potentially large contribution from these terms is quadratic in Λ and arises from the longitudinal components of the $W^\pm$ propagators in fig. 7. To estimate the decay rate we should take matrix elements between the K_L state and the vacuum and use PCAC. Once we do that the leading λ_i contributions quadratic in Λ vanish. This follows from the fact that

$$\langle 0 | \bar{v}(d)\gamma^\mu(1-\gamma_5)u(s) | K_L \rangle = \sqrt{2} f_K q_K^\mu \tag{40}$$

and $q_K^\mu p^\alpha p'^\beta \Delta V_{\alpha\beta\mu} = 0$ (as can be seen from straightforward kinematics). Here q_K^μ is the momentum of the K_L meson, p^α and p'^β are the momenta of the intermediate charged weak bosons and $\Delta V_{\alpha\beta\mu}$ is the piece of the ZWW vertex containing the λ_i terms.

Thus, we are left to consider only the effects on $K_L \to \mu\mu$ from the Δf_1 and Δf_2 pieces in eq. (32). The amplitude associated to these pieces is explicitly calculated to be,

$$\Delta T = -i\frac{G_F}{\sqrt{2}} \sin\theta_c \cos\theta_c \left[\frac{\alpha}{\pi}\right] \bar{\epsilon}\, \tfrac{1}{2}\bar{v}_d(p')\gamma^\mu \tfrac{1}{2}(1-\gamma_5) \times$$

$$\times\, u_s(p)\bar{u}(p_-)\gamma_\mu(a - b\gamma_5)v(p_+) \tag{41}$$

where a and b are given by eqs. (4b) and (4c), Δf_{12} is as eq. (33b) and $\bar{\epsilon}$ is a shorthand for

$$\bar{\epsilon} \equiv \frac{(m_c^2 - m_u^2)}{4M_W^2 \tan^2\theta_W} \Delta f_{12} \frac{\Lambda^2}{M_W^2} \tag{42}$$

Applying PCAC we obtain

$$T(K_L \to \mu\mu) = -\frac{iG_F}{2} m_\mu \frac{\alpha}{\pi} \bar{\epsilon} \sin\theta_c \cos\theta_c f_K \bar{u}(p_-)\gamma_5 v(p_+) \tag{43}$$

In order to reduce the theoretical uncertainties associated with the previous calculation, we shall compare our results for the ratio,

$$R = \frac{\Gamma(K_L \to \mu\mu)}{\Gamma(K_L \to \gamma\gamma)} \qquad (44)$$

with the corresponding experimental number.

Experimentally we know,

$$R < 2.44 \times 10^{-5} \qquad (45)$$

The amplitude eq. (43) should interfere with the amplitude in fig. 6 (which gives the bulk of the $K_L \to \mu\mu$ rate). This latter amplitude has been thoroughly studied in the literature. We refrain from giving its explicit form [9]. Instead, we give our final result for R (eq. (44)) which incorporates the effect of both amplitudes. After some numerical elaboration R finally reads,

$$R = (609\bar{\epsilon}^2 + 54\bar{\epsilon} + 1.2) \times 10^{-5} \qquad (46)$$

When contrasted with the experimental value eq. (45) and using eq. (42) gives

$$-2\left|\frac{1\text{TeV}}{\Lambda(\text{TeV})}\right|^2 < \Delta f_{12} < .3\left|\frac{1\text{TeV}}{\Lambda(\text{TeV})}\right|^2 \qquad (47)$$

Unfortunately this constraint is very poor.

6.- SUMMARY

Despite the general success of the standard electroweak model, there are strong theoretical reasons to believe that new physics must emerge at the ~1 TeV energy scale. If this new threshold is related to deeper layers of substructure, i.e. quarks and/or gauge bosons are composite objects, then the pointlike structure of the couplings should be a good approximation only up to distances large on the scale of Λ^{-1}. In particular, the self-couplings of the intermediate vector bosons should show, to some extent, deviations from their standard model form. It will require energies on the order of 160 GeV to probe the nature of the γWW and ZWW interactions (at e^+e^- machines). Nevertheless, one

can infer useful constraints on those interactions from existing low energy data.

In the preceding sections we have undertaken a thorough analysis of the bounds imposed on the electromagnetic interactions of the charged weak boson $W^\pm$ and/or on the interaction of the neutral Z° boson coupled to the charged weak bosons $W^\pm$ by the experimental data on the parameter ρ and on the process $K_L \to \mu\mu$. We have been very careful in exactly identifying the true manifestations of substructure in the divergent loop integrals. Indeed, naïve evaluation of the effects of substructure on the ρ parameter by previous work led to a spurious behaviour in the cut-off (Λ^4 dependence) which in turn implied a too restrictive bound on the anomalous magnetic moment of the charged weak boson. Proceeding as explained in section 2 we established a milder (quadratic) dependence on Λ and hence a much weaker constraint on the magnetic moment.

The interactions of photons and neutral intermediate bosons with charged weak bosons have been described symmetrically in sections 2 and 3. Specifically, in section 3 we derived bounds on arbitrary magnetic dipole moments and electric quadrupole moments of the $W^\pm$ boson . We observe that present data tolerate substantial departure from the $SU(2)\times U(1)$ gauge structure of the couplings.

Since the neutral weak boson Z° is, of course, far less understood (both experimentally and theoretically) than the photon, one may question to a greater degree its nature and interactions. So, in sections 4 and 5 we allowed for more free parameters in the ZWW vertex. The new degrees of freedom introduced, however, turned out to be fairly constrained by the experimental data on the parameter ρ. ($K_L \to \mu\mu$, on the contrary, was shown to provide no useful bounds at all).

Obviously, an increased experimental accuracy would give better bounds and constrain still further the a priori possible manifestations of compositeness. Thus, performing improved

low energy experiments* can provide information which otherwise would require very high energy colliders.

One of us (S.P.) is very grateful to Salvador Orteu for his help in the computing.

*.- See ref. (10) for a very exhaustive analysis, using an effective Lagrangian approach, of possible effects (other than those discussed here) due to new interactions.

TABLE 1

3-vertex

$$V[W_\alpha(p),W_\beta(p'),i_\mu(q)]=ig_i\{g_{\alpha\beta}(p+p')_\mu-g_{\alpha\mu}(p-q)_\beta-g_{\beta\mu}(p'+q)_\alpha+$$

$$+\Delta\chi_i(g_{\alpha\mu}q_\beta-g_{\beta\mu}q_\alpha)+\frac{\lambda i}{M_W^2}[g_{\alpha\beta}(p.qp'-p'.qp)_\mu-g_{\alpha\mu}(p.p'q-p'.qp)_\beta-$$

$$-g_{\beta\mu}(p.qp'-p'.pq)_\alpha+p_\mu p_\alpha q_\beta-p'_\mu q_\alpha p_\beta]\}$$

4-vertices

$$V[W_\alpha(p),W_\beta(p'),i_\mu(q),j_\nu(q')]=-ig_ig_j(2g_{\mu\nu}g_{\alpha\beta}-g_{\alpha\mu}g_{\beta\nu}-g_{\alpha\nu}g_{\beta\mu})+$$

$$+ig_ig_j\frac{(\lambda_i+\lambda_j)}{2M_W^2}(g_{\mu\nu}g_{\alpha\beta}(q-q').(p'-p)-g_{\alpha\mu}g_{\beta\nu}(q.p'+q'.p)+$$

$$+g_{\alpha\nu}g_{\beta\mu}(q.p+q'.p')-g_{\alpha\beta}[q_\nu(p'-p)_\mu-q'_\mu(p'-p)_\nu]+g_{\mu\nu}[p_\beta(q-q')_\alpha-$$

$$-p'_\alpha(q-q')_\beta]+g_{\beta\nu}(q_\alpha p'_\mu+q'_\alpha p_\mu+q'_\alpha p'_\mu-q'_\mu p'_\alpha)-g_{\alpha\nu}(q'_\beta p_\mu-q'_\mu p_\beta+$$

$$+q_\beta p_\mu+q'_\beta p'_\mu)-g_{\mu\beta}(p'_\nu q_\alpha-p'_\alpha q_\nu+p_\nu q_\alpha+p'_\nu q'_\alpha)+g_{\mu\alpha}(p_\nu q_\beta-p_\beta q_\nu+q_\beta p'_\nu+q'_\beta p_\nu)\}$$

$$V[W_\alpha(p),W_\beta(p'),W_\mu(q),W_\nu(q')]=ig_\gamma^2(2g_{\beta\nu}g_{\alpha\mu}-g_{\beta\alpha}g_{\mu\nu}-g_{\beta\mu}g_{\nu\alpha})+$$

$$+ig_\gamma^2(2\Delta\chi_\gamma+\Delta\chi_\gamma^2)(2g_{\beta\nu}g_{\alpha\mu}-g_{\beta\alpha}g_{\mu\nu}-g_{\beta\mu}g_{\nu\alpha})-ig_\gamma^2(1+\Delta\chi_\gamma)\frac{\lambda_\gamma}{M_W^2}\{g_{\nu\beta}g_{\mu\alpha}\times$$

$$\times(q'+p').(q+p)-g_{\nu\alpha}g_{\mu\beta}(q.q'+p.p')-g_{\alpha\beta}g_{\mu\nu}(p'.q+q'.p)+g_{\mu\nu}(q'_\beta q_\alpha-$$

$$-q'_\alpha q_\beta+q_\beta p'_\alpha+q'_\alpha p_\beta)+g_{\alpha\beta}(p_\nu q'_\mu+p'_\mu q_\nu+p'_\nu p_\mu-p'_\mu p_\nu)-g_{\mu\alpha}(q_\beta p'_\nu+p_\nu q'_\beta+$$

$$+q_\nu q'_\beta+p_\beta p'_\nu)-g_{\nu\beta}(p'_\mu q_\alpha+q'_\alpha p_\mu+q'_\mu q_\alpha+p'_\alpha p_\mu)+g_{\mu\beta}(p'_\nu q_\alpha-p'_\alpha q_\nu+q_\nu q'_\alpha+$$

$$+p'_\alpha p_\nu)+g_{\alpha\nu}(q'_\beta p_\mu-q'_\mu p_\beta+p_\beta p'_\mu+q'_\mu\ q_\beta)\}+(\gamma\leftrightarrow Z)$$

TABLE CAPTION

Table 1.- Feynmann rules for the 3 and 4 vertices, derived from eqs. (10-13) in section 2. Momenta p and q enter the vertex and momenta p' and q' leave the vertex. i,j=Z,γ.

FIGURE CAPTIONS

Fig. 1.- Contributions of vector boson self-couplings to vacuum polarization.

Fig. 2.- Vacuum polarization and vertex correction diagrams contributing to δ_i.

Fig. 3.- Allowed values (shaded area) of $\Delta\chi_\gamma$ and $\Delta\chi_Z$ for a compositeness scale Λ=1 TeV.

Fig. 4.- Allowed values (shaded area) of λ_γ and λ_Z for a compositeness scale Λ=1 TeV.

Fig. 5.- Allowed values (shaded area) of Δf_1 and Δf_2 for a compositeness scale of Λ=1 TeV.

Fig. 6.- Diagram for $K_L \to \gamma\gamma \to \mu\mu$.

Fig. 7.- Diagram contributing to $K_L \to \mu\mu$ and involving the vertex ZWW.

REFERENCES

1.- F. Herzog, Phys. Lett. 116B (1984) 264 ; M. Suzuki, Phys. Lett. 153B (1985) 289; A. Grau and J.A. Grifols, Phys. Lett. 154B (1985) 283; J.C. Wallet, Phys. Rev. D32 (1985) 813.

2.- A. Grau and J.A. Grifols, Phys. Lett. 166B (1986) 233.

3.- J. van der Bij, private communication.

4.- A. Grau and J.A. Grifols, Phys. Lett. 154B (1985) 283.

5.- M. Suzuki, Phys. Lett. 153B (1985) 289.

6.- F. Antonelli, M. Consoli and G. Corbó, Phys. Lett. 91B (1980) 90 and Nucl. Phys. B183 (1981) 195; M. Veltman, Phys. Lett. 91B (1980) 95.

7.- H. Aronson, Phys. Rev. 186 (1969) 1434.

8.- M.K. Gaillard and B.W. Lee, Phys. Rev. D10 (1974) 897; M.K. Gaillard, B.W. Lee and R.E. Shrock, Phys. Rev. D13 (1976) 2674.

9.- L. Bergström, Z. Phys. C14 (1982) 129.

10.- W. Buchmüller and D. Wyler, Nucl. Phys. B268 (1986),621.

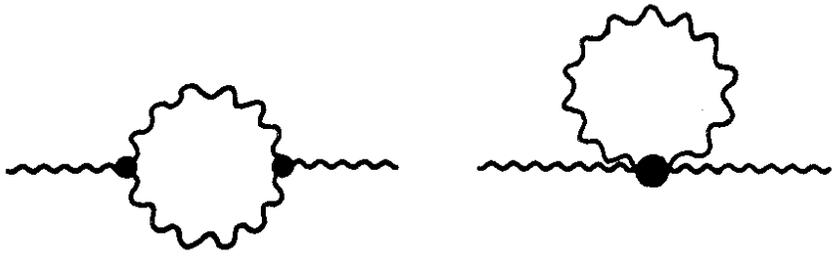

Fig 1

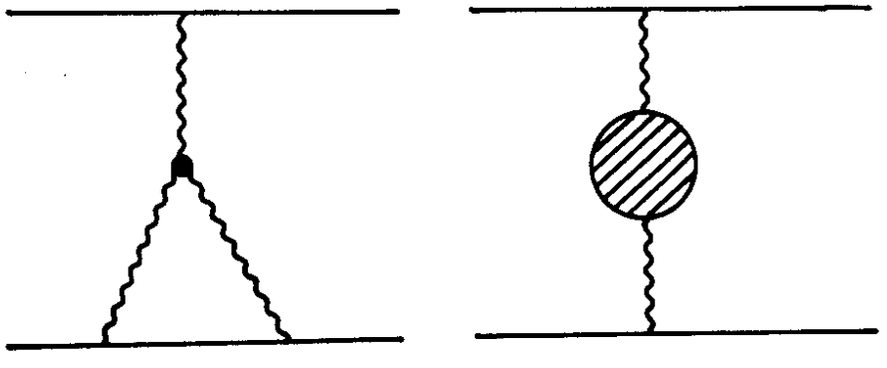

Fig 2

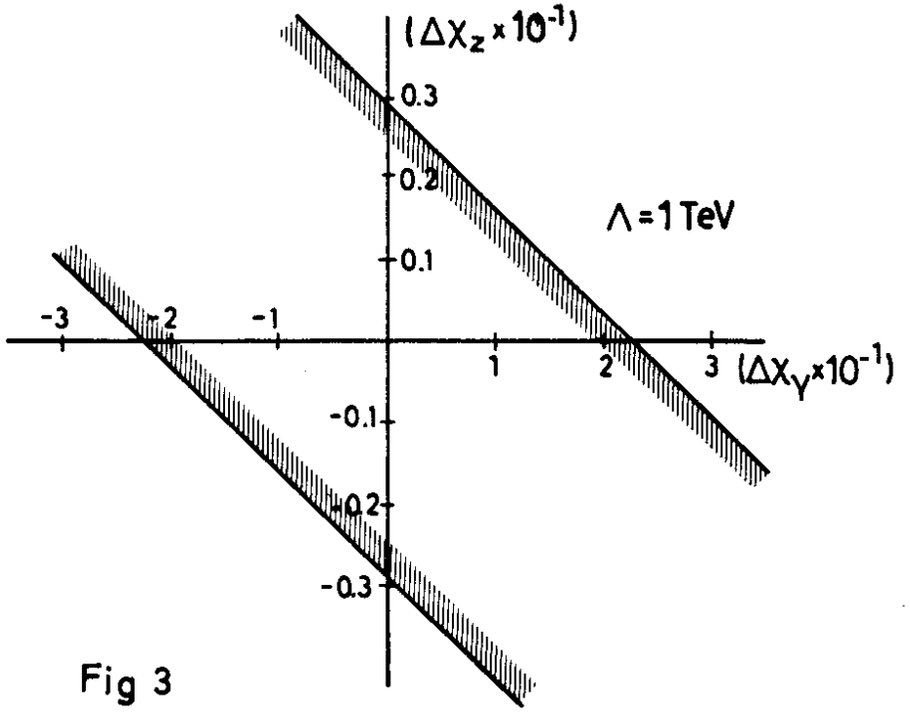

Fig 3

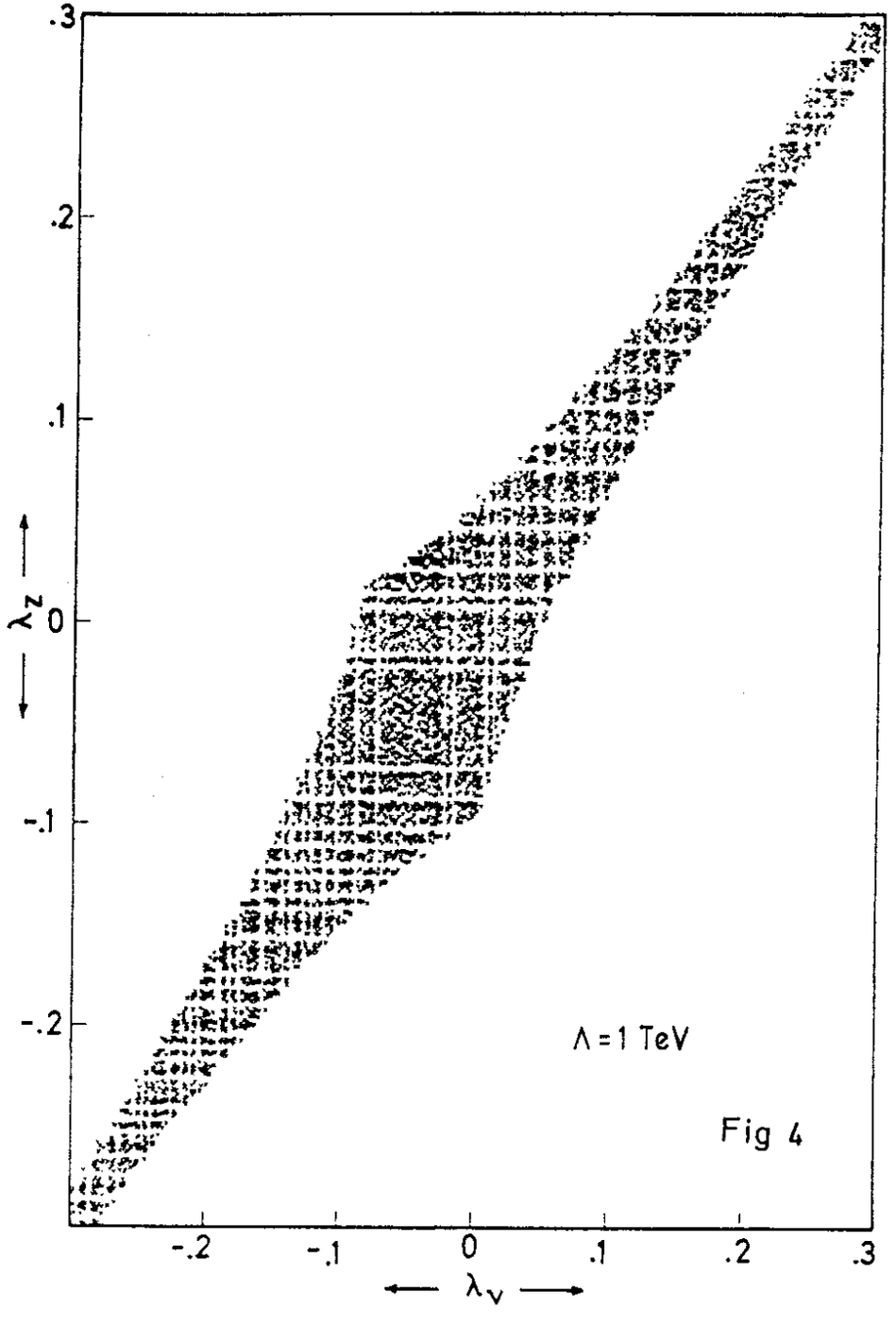
.3
.2
.1
0
-.1
-.2
λ_Z
-.2
-.1
0
.1
.2
.3
λ_γ
Λ = 1 TeV

Fig 4

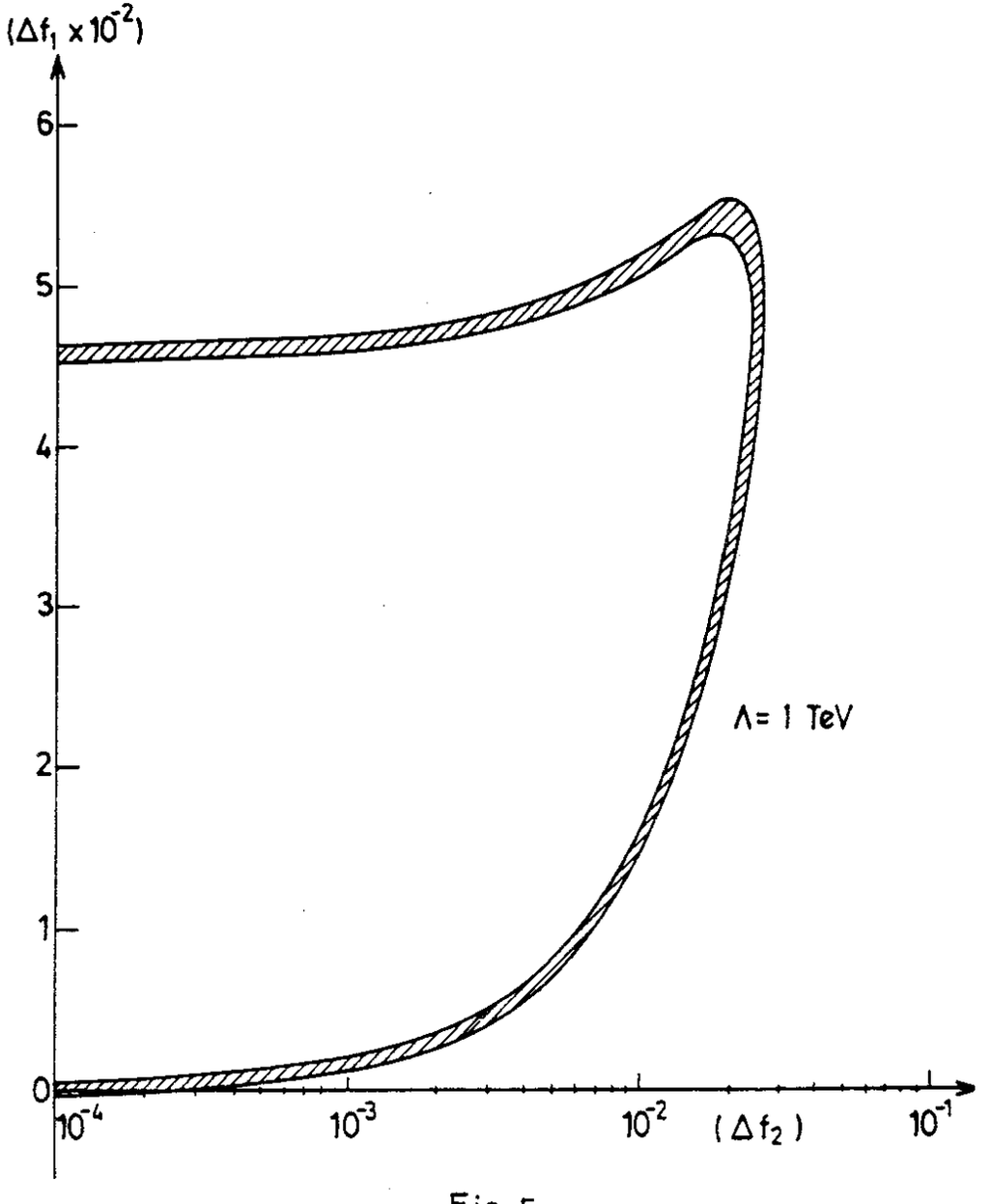
$(\Delta f_1 \times 10^{-2})$
6
5
4
3
2
1
0
10^{-4}
10^{-3}
10^{-2}
(Δf_2)
10^{-1}
Λ = 1 TeV

Fig 5

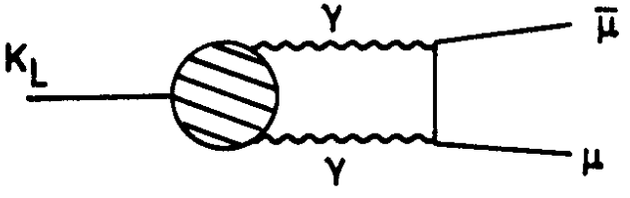

Fig. 6

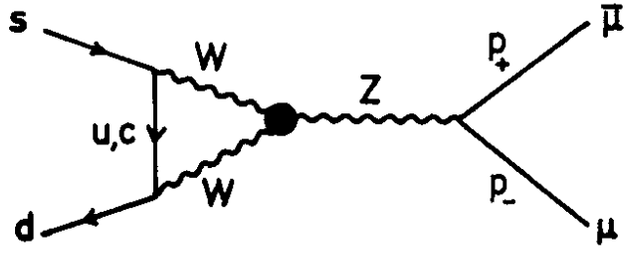

Fig. 7